Effect of Rock Heterogeneity and Relative Permeability on CO_2 Flow in Brine-Saturated Berea Sandstone

Ljubinko Miljkovic

Abstract A general consensus has been reached in the scientific community that large-scale anthropogenic emission of CO_2 will continue to cause global warming of the earth's lower atmosphere, which is expected to have the secondary effects of raising sea level, disrupting ecosystems, and increasing summer lengths, intensities, and heat-related mortality. One potential recourse is carbon-capture and sequestration (CCS) technology, which separates CO_2 from the exhaust gas of fossil fuel burning electricity plants and stores it as a compressed supercritical fluid in deep saline aquifers. Existing CCS field experiments have failed to produce reservoirs of high CO_2-saturation, and rock heterogeneity (spatial variations in rock permeability) is thought to be the cause. A greater understanding of the effect of heterogeneity on the saturation of CO_2 is needed to better understand CO_2 storage capacity. The research presented in this paper compares two TOUGH2 simulations of injected CO_2 into a brine-saturated Berea sandstone core: one heterogeneous and the other homogeneous. Small, unstructured heterogeneity was found to have no impact on CO_2 saturation. Further, this research determined experimentally the relative permeability curves for CO_2 and brine in the heterogeneous Berea sandstone core using standard core-flooding techniques. The measured relative permeability data were then characterized and input into a TOUGH2 numerical simulation of a homogeneous core to simulate the effects of heterogeneity. A homogeneous simulation was used to determine if such computationally simpler simulations, given proper relative permeability data, could simulate the behavior of more complex, heterogeneous experiments. Indeed, this enhanced model accurately simulated average CO_2 saturation of the Berea core to within 2%, though the cross-sectional CO_2 saturation profile differed due to localized variability in the Berea core.

Introduction

Over the past several hundred years, atmospheric concentrations of CO_2 have risen steadily to 380 ppm at the present time, up from pre-industrial 280ppm levels. This elevation is due primarily to the large-scale burning of fossil fuels such as coal, natural gas, and petroleum for electricity generation, transportation, and other human energy services (Benson 2005). Today, anthropogenic sources release approximately 6.5 gigatonnes (Gt) of carbon into the atmosphere every year, chiefly in the form of CO_2. The elevated levels of CO_2 and other greenhouse gases have increased the atmosphere's ability to reabsorb reflected infrared (IR) radiation from the earth's surface, resulting in a warming of the planet. If unmanaged emissions of fossil carbon continue, a significant increase in mean global surface temperature of between 1.5 ^{o}C and 4.5 ^{o}C is expected by the end of the 21st century (Wuebbles et al. 1999). The effects of global warming have already been observed in the melting of polar icecaps and sea-level rise. Further, the hydrologic cycle is expected to intensify with more precipitation in some areas, while mid-latitude regions should experience drying and drought (Hayhoe et al. 2004, Wuebbles et al. 1999).

Though there are many sources of anthropogenic CO_2 as well as many opportunities for mitigation, the electricity generation sector in particular offers a logical place to explore alternative approaches because it is made up of relatively few, large sources – unlike the transportation sector, which is made up of many dispersed CO_2 emitters. In addition, the Intergovernmental Panel on Climate Change's (IPCC) model that describes the effects of unabated economic growth, called the "Business as Usual" model, indicates that global emissions from this sector will rise dramatically by 2020, from 7.7 $GtCO_2$/year to 15 $GtCO_2$/year, offering an opportunity for non-carbon-emitting energy technologies to make a significant impact (IPCC 2001).

Several major low- or zero-carbon intensity electricity generation options are being considered for increased deployment in the United States, such as nuclear fission, photo-voltaic panels, wind turbines, increased natural gas burning, and integrated gasification combined cycle (IGCC) coal burning with carbon capture and sequestration (CCS) (Beck 1999, van der Zwaan and Rabl 2004). In this research, I examine carbon capture and sequestration, a non-carbon-emitting energy technology.

Carbon capture and sequestration is a process that separates CO_2 from industrial and power-

sector sources, transports it to an isolated site, and injects it into deep subsurface geologic formations for long-term isolation from the atmosphere. There are currently three demonstration CCS projects around the world, one of which has been operating for nearly ten years (Benson 2005). Future CCS sites are being planned to inject supercritical CO_2 into deep sandstone salt-water aquifers, whose abundance and proximity to existing CO_2 sources makes them attractive reservoirs. For this technology to expand enough to contribute significantly to our climate change mitigation strategy, more research is needed to better understand subsurface CO_2 transport during and after injection to help better characterize a site's capacity, longevity, and stability.

This study will concern itself with predicting the storage capacity of saline formations and the size of underground plumes of injected CO_2. Both of these factors are largely controlled by two features of a storage formation: the natural variability (heterogeneity) of the rock and the relative permeability of the rock to CO_2. Localized variability of permeability[1] in natural rock – hereafter called rock heterogeneity – makes CO_2 (or other fluid) flow through it very difficult to predict accurately because of the lack of precise heterogeneity characterization information and because fluids tend to channel through paths of higher permeability in porous materials (Scheidegger 1974). Additionally, when two fluids are present, such as brine (salt-water) and CO_2 in this case, the relative permeability[2] of each fluid indicates how easily and to what extent one fluid can be displaced by another. Relative Permeability data are necessary for accurate models of flow through heterogeneous rock and capacity predictions.

Relative permeability is a multiplier (between 0 and 1) of intrinsic permeability[3] which describes the relative ease of flow of two competing fluids, such as CO_2 and brine, through a porous medium. In addition, relative permeability of a fluid increases proportionally with the saturation[4] of that fluid in the rock pores. Although some CO_2 does dissolve in the brine, most of the CO_2 exists as a separate phase. It is the proportion of pore space that the non-dissolved CO_2

---

[1] Permeability refers to the difficulty with which one or more fluids passes through the porous rock.

[2] Relative permeability is a ratio of effective permeability of a single fluid at a particular saturation to the intrinsic permeability of that fluid when it is the only fluid present. If a single fluid is present in a rock, its relative permeability is 1.0. Calculation of relative permeability allows comparison of the different abilities of fluids to flow in the presence of each other, since the presence of more than one fluid generally inhibits flow. The sum of two fluids' relative permeabilities need not equal 1.0, since the fluids may interfere with each other.

[3] Intrinsic permeability is the permeability of a porous substance to a single fluid.

[4] Unlike the saturation of a solute in a solvent, in this paper saturation refers to the percent of the pore-space occupied by either CO_2 or brine. A brine-saturated core, therefore, has all its pore-space filled with brine.

phase occupies that is relevant to relative permeability calculations.

Numerical simulation of CO_2 injection is an essential tool for determining a site's capacity as well as predicting how far a plume of injected CO_2 will extend below ground. The current problem with field-scale simulations is that they do not take accurate account of heterogeneity of the rock because such small-scale heterogeneity cannot be measured at the field scale.

This study uses a small cylindrical core (3.81cm x 7.7cm) of Berea sandstone. Since it is a material present in a significant number of saline aquifers of interest to CO_2 injection, it was chosen as the study medium to investigate CO_2 flow. Berea has a typical porosity of 20% to 30% that remains fairly constant through space. The chosen core, however, poses small unstructured variations of permeability. Two characteristics affect the movement of CO_2 through brine-saturated rock: rock heterogeneity and relative permeability of CO_2 and brine. This study pays due diligence to these fundamental principles of fluid flow through porous media and provides grounding for future studies of highly heterogeneous rocks of various types.

This study is designed to explore the hypothesis that rock heterogeneity leads to less effective displacement of water by injected CO_2 and thus a decrease in CO_2 saturation. Second, this study will collect heretofore unmeasured relative permeability data from typical reservoir rock and, through numerical simulation, predict measured CO_2 saturation changes across the core.

Methods

The first part of the study compares two simulated CO_2 injection experiments: one with a heterogeneous core (with the same distribution of porosity and permeability as the Berea core) and the other with a homogeneous core. The homogeneous core has porosity and intrinsic permeability set to the average values of the heterogeneous core. I used the TOUGH2 multi-phase simulator to model both injections of CO_2 at a pressure of 6.89MPa and rate of 0.5mL/min for three hours. All other input parameters we identical for both models.

To reflect the heterogeneity of the Berea core in the heterogeneous model, the precise spatial distribution of porosity and permeability found in the real Berea core were measured. A Siemens

medical computer-tomography[5] (CT) scanner was used to scan 25 3mm "slices" of the dry Berea core along its length, producing 25 images of the core's interior. The various shades of darkness of the images indicate the level of beam attenuation. Since rock attenuates x-rays more strongly than air, areas of higher porosity appeared darker and visa versa. We scaled the raw data within these 25 images to represent the distribution of porosity of the core. The scanner produces images with a resolution of 0.4mm laterally, and 3mm along the length of the core.

To generate 25 images representing the core's intrinsic permeability distribution, the above porosity images were digitally processed using the Kozeny-Carmen equation, which converts porosity data from each CT scan slice into an equal number of intrinsic permeability measurements:

$$K_j \ ? \ \frac{f_j^3}{3.42 \ ? \ 10^{10}(1 \ ? \ f_j)^2}$$

where K_i is a single measure of permeability (m^2) and f_j is a single measure of porosity (Hillel 1980). The numerical constant (3.42×10^{10} m^{-2}) is specific to the Berea core in use, which has an average intrinsic permeability of 270×10^{-15} m^2 and a porosity of 0.23.

To prepare the porosity and permeability data for the TOUGH2 simulation, the resolution of both the porosity and permeability images was digitally "coarsened" by taking spatial averages of the images to produce a 3D map composed of 1 x 1 x 3mm "cells." Each cell thus defined a discrete segment of the core with a single value of porosity and permeability. These 32,400 cells represent a map of the core which is input into TOUGH2 as the material through which TOUGH2 simulates CO_2 injection[6].

The second part of the study determined experimentally, and verified by simulation, the relative permeability of CO_2 and brine in the Berea core. To determine relative permeability, seven different proportions of CO_2 and brine were injected into a brine-saturated core at in-situ pressure and room temperature (see Table 1). During each trial, the saturation of CO_2 and brine in the core was equilibrated and measured. Each steady-state saturation value was then

[5] Computer tomography is a technique for displaying a representation of a cross-section through a solid object using X-rays.

[6] Unfortunately, with the computer resources available to me, it is currently not possible to create a simulation with the same resolution as the CT images.

correlated with the corresponding measured relative permeability value for CO_2 and brine, calculated by Darcy's Law. These value pairs were then plotted to form the relative permeability curves for CO_2 and brine.

A core-flooding apparatus (described in Appendix B) similar to that used by Geffen (1952) was used to inject liquid CO_2 and brine into the same end of the horizontally oriented Berea core. A confining pressure of 9.65MPa was applied to the core within an aluminum core-holder to simulate reservoir conditions. A series of piston pumps delivered brine (0.5M KI) and CO_2 pressurized at 6.89MPa at a total rate of 3mL/minute during each of the 7 trials. Each trial proceeded at a different ratio of CO_2 to brine (see Table 1).

Table 1: Volumetric proportions of CO2 and brine for each trial in the relative permeability curve determination.

	Trial 1	**Trial 2**	**Trial 3**	**Trial 4**	**Trial 5**	**Trial 6**	**Trial 7**
% CO_2	5%	10%	20%	50%	80%	90%	95%
% Brine	95%	90%	80%	50%	20%	10%	5%

During each trial, the pressure drop[7] across the core was measured by a pressure transducer connected to a computer, and the computer recorded the data. Based on the flow rate for each fluid, I used Darcy's Law to determine the effective permeability[8] of the whole core for each fluid in each trial:

$$K_n ? \frac{q ? L ? ?}{A ?? P_n}$$

where K_n is effective permeability of a single fluid (m^2) in trial n, q is flow rate of a single fluid (m^3/s), L is core length (m), A is the cross-sectional core area (m^2), μ is viscosity of a single fluid (Pa· s), and $?P_n$ is the pressure drop across the core (Pa) in trial n (Collins 1961). To calculate

[7] Pressure drop is the difference between the pressure at the end of the core at which CO_2 is injected (the inlet) and the end at which CO_2 exits the core (the outlet). Pressure drop is related to the injection rate of CO_2 and the permeability of the core.

[8] Effective permeability is the permeability of a porous substance to a single fluid when two fluids are present. The sum of the effective permeabilities of two fluids does not have to equal the intrinsic permeability of the core, as the

the relative permeabilities of CO_2 and brine for each trial, I divided each fluid's effective permeability by the core's average intrinsic permeability (K_i) , 270×10^{-15} m^2, which was measured using Darcy's law by flowing only water through the core. The following equations clarify:

$$K_{H_2O,R} \ ? \ \frac{K_{H_2O}}{K_i} \qquad , \qquad K_{CO_2,R} \ ? \ \frac{K_{CO_2}}{K_i}$$

where $K_{H2O,R}$ and $K_{CO2,R}$ are the relative permeability of brine and CO_2 respectively, K_{H2O} and K_{CO2} are the effective permeability of brine and CO_2 calculated by Darcy's Law, and K_i is the average intrinsic rock permeability (Hillel 1980).

To construct the desired relative permeability curves[9] for brine and CO_2, precise saturation values for each fluid at equilibrium were needed. Equilibrium for each trial was reached once intermittent CT scans of the core showed that the spatial distribution of brine and CO_2 did not change with continued injection. Once the fluids were equilibrated, a series of CT scans was taken along the length of the core to measure the brine and CO_2 saturation. Relative permeability curves were constructed by graphing two curves: brine relative permeability and CO_2 relative permeability, both plotted against brine saturation.

A numerical simulation of the above experiment was run to verify the accuracy and reliability of the TOUGH2 simulation system in use. However, instead of a heterogeneous core, a core of homogeneous permeability and porosity was used, similar to the one in the homogeneous simulation above. This simulation differed from the one performed above in that the measured relative permeability values obtained in the lab experiment were input into this homogeneous model. The saturation profiles at several injection proportions were compared to verify TOUGH2's ability to simulate the lab experiment.

To input the relative permeability data from the lab experiment into the homogeneous simulation, parameters of a common power-law function of relative permeability were determined by trial and error to produce a best-fit function to the collected data. Appropriate parameter values were found by trial and error to define a relative permeability function of brine

---

fluids impede each others' flow.

[9] Relative permeability curves are the graphs of relative permeability data of two competing fluids (in this case CO_2 and brine) plotted against the saturation of one of the fluids. The relative permeability of a fluid increases with the saturation of that fluid.

and CO_2. These functions define a relative permeability curve for each fluid given brine saturation, CO_2 saturation, the residual brine saturation[10], and a best-fitting exponent for each curve:

$$K_{H2O,R} = \left(\frac{S_{brine} - S_{brine,r}}{1 - S_{brine,r}}\right)^{N_{brine}}, \quad K_{CO2,R} = \left(\frac{1 - S_w}{1 - S_{wr}}\right)^{N_{CO2}}$$

where $K_{H2O,\ R}$ and $K_{CO2,\ R}$ are the relative permeability of brine and CO_2 respectively, S_{brine} is brine saturation, $S_{brine,r}$ is residual brine saturation, N_{H2O} is the brine function exponent, and N_{CO2} is the CO_2 function exponent. These functions and the appropriate parameters were then input into the homogeneous TOUGH2 model to more accurately describe the permeability of each fluid at different saturations in the Berea core used in the lab experiment. This information is vital to accurately recreating physical flow experiments with a simulation. The goal in this section was to reproduce the saturation profile from the lab experiment, which uses a heterogeneous core, with a homogeneous model defined with the experimentally determined relative permeability.

Because this simulation measures the relative permeabilities of CO_2 and brine, which are defined explicitly in the model itself, reproduction of these data serves merely to build confidence about the internal consistency of the model. However, the saturation profile of the core at equilibrium is never defined in the input. It was measured independently.

Results

Rock heterogeneity is of great interest to CCS because it is expected to cause channeling of CO_2 through areas of higher permeability, bypassing lower permeability zones of the rock, thus decreasing the rock's total storage capacity. In the first part of this study, I compared a homogeneous and heterogeneous TOUGH2 simulation of CO_2 injection into a brine-saturated core to investigate the effect of heterogeneity on CO_2 saturation. Next, I experimentally determined the relative permeability of CO_2 and brine in the brine-saturated Berea core. Functions and appropriate parameters that were fit to the data were input into a simulation of the physical experiment. The simulation results were then compared to the physical experiment

[10] Residual brine saturation is the saturation of brine that remains in the core when only CO_2 is being injected. It is the saturation at which brine becomes immobile, unable to be moved by additional CO_2 injection.

results to evaluate the simulation's ability to predict the real experiment and verify TOUGH2's internal consistency.

To define the permeability variations of the Berea core in the heterogeneous TOUGH2 simulations, the CT images of the core were digitally "coarsened." Lower the resolution of the data helped speed up simulation time. As a result, however, detailed structural features were lost. This was not a concern, however, since the general shape and size of the features were retained in the coarsened images.

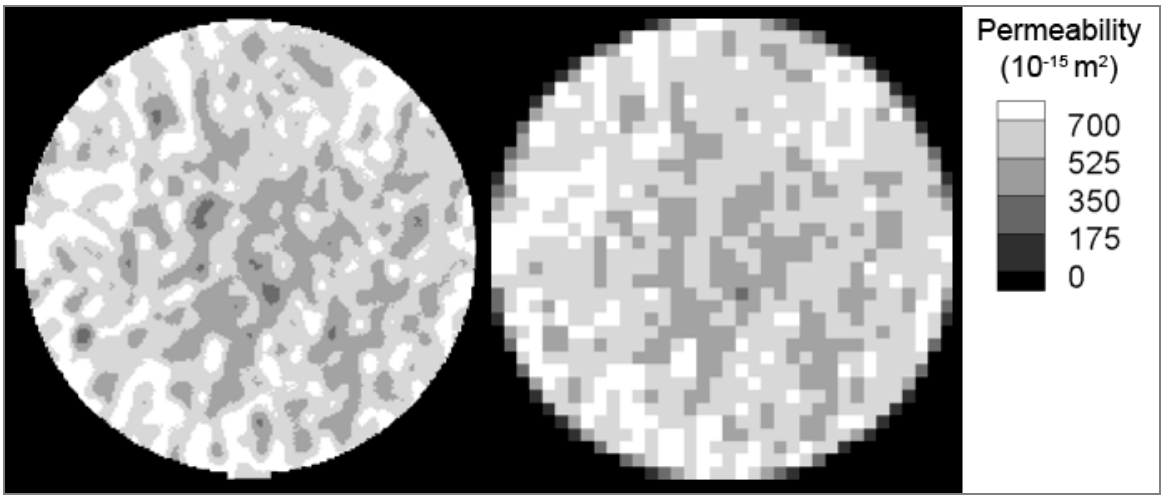

Figure 1. The coarsened image loses much of the detailed permeability information. However, the general structure of heterogeneity, which is what is relevant to this study, remains.

To determine the effect of heterogeneity on CO_2 saturation within the simulated cores, the CO_2 saturation profiles of each simulation were compared at various times. Both simulations produced very similar CO_2 saturation profiles, differentiated only by small localized variations in the heterogeneous simulation.

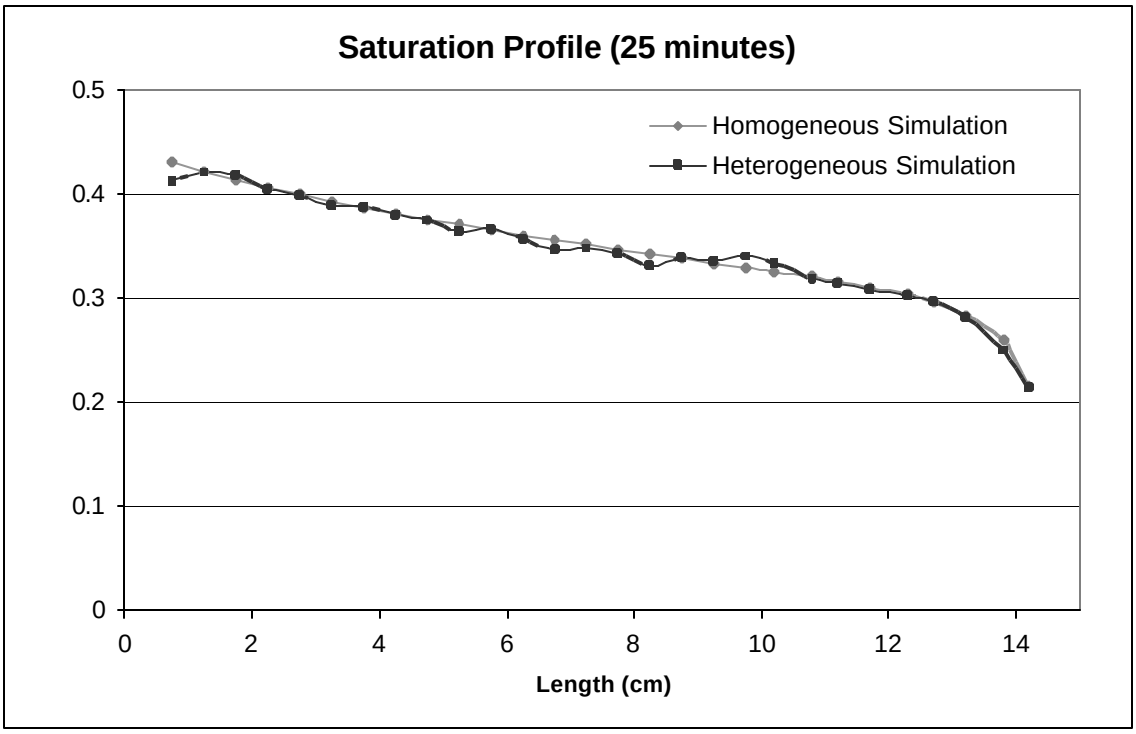

Figure 2. Profile of CO_2 along the length of the simulated core at 25 minutes into the simulation. Each point is an average of all the "cells" in that slice. Brine saturation is not graphed as it is simply one minus the CO_2 saturation.

The shape of the profile and the mean value of CO_2 saturation within the rock are nearly identical between the two simulations, differing by less than 1%. The permeability variations defined in the heterogeneous simulation seem not to affect rock saturation of injected CO_2.

The relative permeability of CO_2 and brine in the Berea core was calculated with Darcy's Law, using the pressure drop data from the physical experiment. These permeability values were plotted against the brine saturation[11] of the core to obtain relative permeability curves for CO_2 and brine.

[11] Brine saturation and CO_2 saturation sum to 1.0, as they are the only two fluids present in the core. Therefore, knowing CO_2 saturation indicates brine saturation. Brine saturation was chosen as the independent variable merely out of convention.

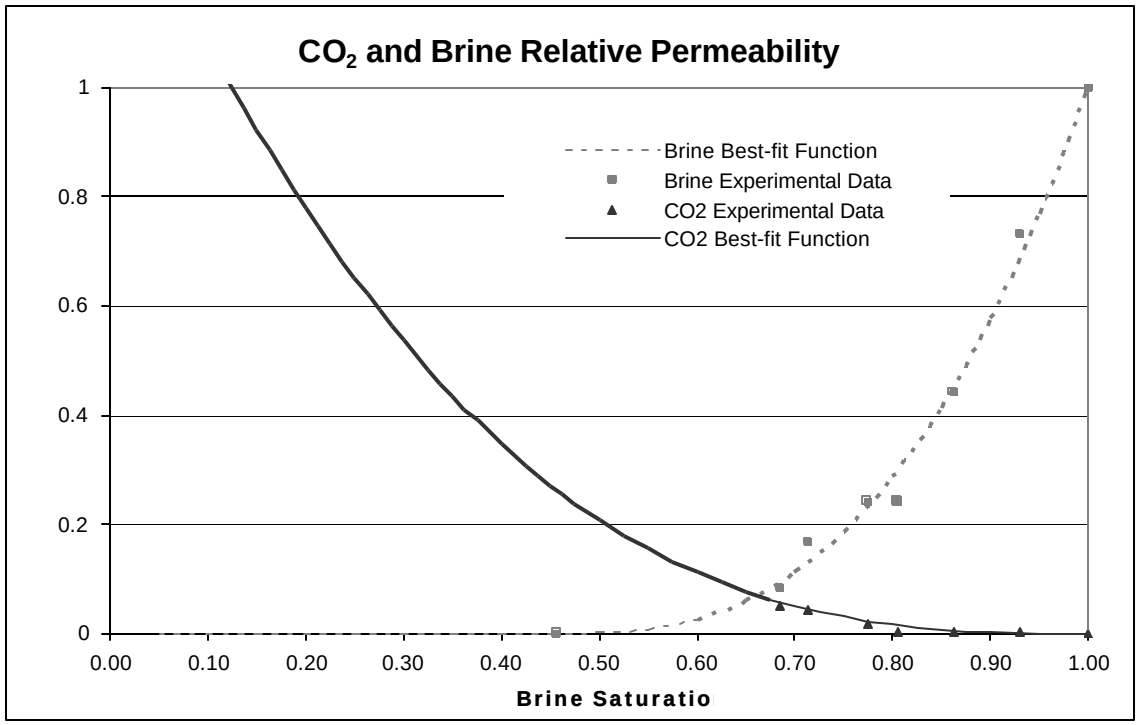

Figure 3. Relative permeability data of brine and CO_2 from physical experiment (calculated using Darcy's law) plotted against brine saturation. Best-fit power-law functions plotted to match data.

Best-fit relative permeability functions for CO_2 and brine were obtained by trial and error by fitting the following two power-law relative permeability functions using the data in Table 2.

$$K_{H2O,R} = \left(\frac{S_{brine} - S_{brine,r}}{1 - S_{brine,r}}\right)^{N_{brine}} \quad , \quad K_{CO2,R} = \left(\frac{1 - S_w}{1 - S_{wr}}\right)^{N_{CO2}}$$

Table 2. Parameter values that produce curves that fit the relative permeability data of the physical experiment.

Residual Brine Saturation	$S_{brine,r}$	0.46
Best-fit Brine Exponent	N_{brine}	2.7
Best-fit CO_2 Exponent	N_{CO2}	2.8

The power-law functions and best-fit parameters were input into a homogeneous TOUGH2 model to indicate the relative permeability of CO_2 and brine at different proportions of CO_2 and brine in the core at any given time.

The homogeneous simulation, enhanced with the above relative permeability functions, was conducted in the same manner as the physical lab experiment. Multiple proportions of CO_2 and brine were injected, the pressure drop measured, and the relative permeability of each fluid calculated using Darcy's law. As with the physical experiment, the calculated relative

permeability values are plotted against average brine saturation in the core for each trial.

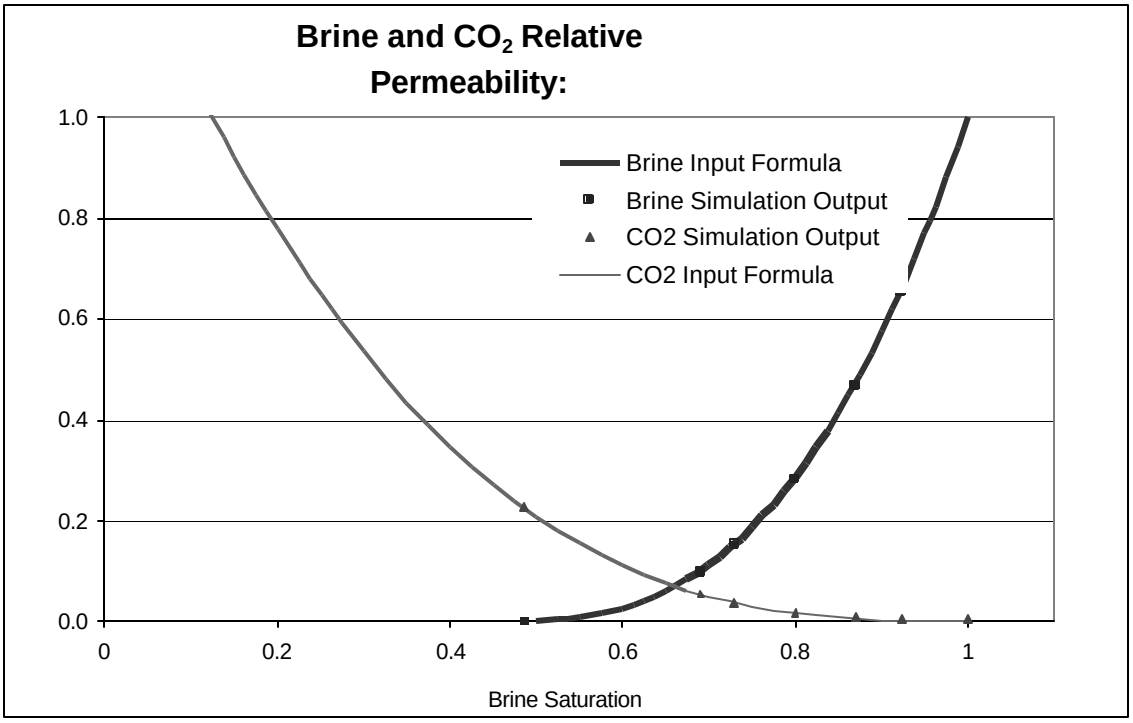

Figure 4. Relative permeability input functions for TOUGH2 model compared to results from simulated relative permeability measurements. Simulation relative permeability measurements are consistent with the relative permeability input curves.

The simulated relative permeability measurements match the functional inputs extremely closely. There is only an average difference of only 1.3% at each data point.

To further investigate the effect of heterogeneity on CO_2 saturation in the core, the experimental and simulated saturation profiles were compared for the 80% CO_2/20% brine injection trial.

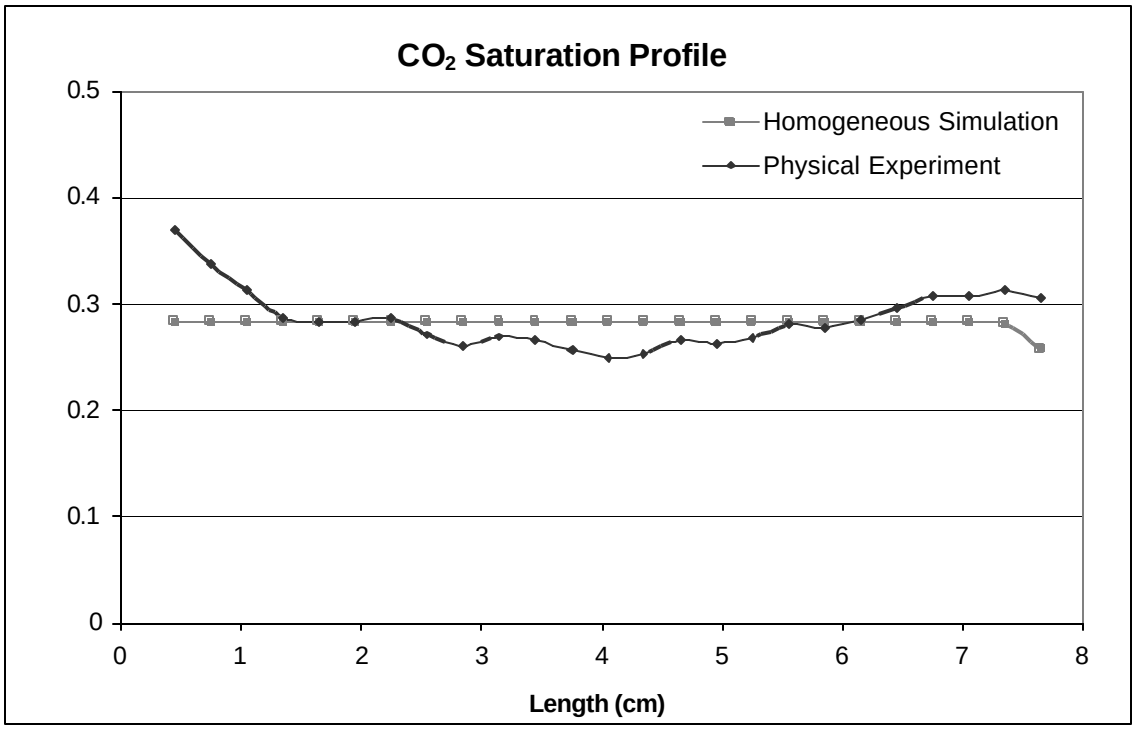

Figure 5. CO_2 Saturation profile for 80% CO_2 injection trial. Variations due to localized heterogeneity are evident, though the average CO_2 saturation is consistent.

Although the results are not as closely matched as between the two simulations in the first part of this study, the average difference is only 1.2%, indicating that the homogeneous model correctly predicts the capacity of this rock. Other injection trials produced similarly consistent results.

Discussion

I compared two simulations which differed only in terms of heterogeneity defined from the sample Berea core. From this, we see that the small, unstructured heterogeneity found in the Berea core does not seem to significantly affect CO_2 saturation. Contrary to the original hypothesis, CO_2 did not form channels through zones of higher permeability, bypassing lower-permeability areas of the core. This result has positive implications for field-scale injection of CO_2 in mildly heterogeneous Berea, as the storage capacity of such rock does not seem to be diminished by small, unstructured heterogeneity. Further research should explore the effect of greater order heterogeneity on CO_2 saturation to determine the relationship between heterogeneity strength and storage capacity. Because this section of the study concerns itself

with numerical simulations, there are very few sources of potential uncertainty within the simulation. The only source of inaccuracy possible is if TOUGH2 is unable to correctly describe the physical processes of a real core injection experiment. This uncertainty factor was explored in the second section of the study.

The relative permeability measurements of the physical and simulated experiments were very similar, indicating the TOUGH2 simulation could accurately describe the interaction of CO_2 and brine in the core given accurate relative permeability curves. Additionally, the simulation's accuracy in reproducing the relative permeability measurements of the input indicates that it is self-consistent and functioning properly.

In terms of the effect of heterogeneity on CO_2 saturation, the core's heterogeneity was shown once again not to have a great effect. When comparing the simulation to the physical lab experiment, greater local variability was observed along the length of the core, however the average CO_2 saturation values were very similar, indicating a similar rock storage capacity. Potential sources of error exist in the pumps used for injection as well as the resolution limitations of the CT scanner. Additionally, material balances could not always be known to a high degree of accuracy since the minute volumes of fluids in the lines between the pumps and the core were ignored. There uncertainties, however, were not very significant because they were small compared to absolute values of numbers. In addition, since only steady-state measurements were taken, short-term flow rate transients, where the effects of these uncertainties is largest, were not important.

Acknowledgments

Thank you to all of my colleagues at Lawrence Berkeley National Laboratory, and particularly: Sally Benson, who mentored me through this research; Liviu Tomutsa, whose laboratory was used for these experiments and whose expertise was invaluable in completing them; and Christine Doughty, who aided in TOUGH2 simulation design and implementation.

References

Beck, P.W. 1999. Nuclear Energy in the Twenty-First Century: Examination of a Contentious Subject. Annual Review of Energy and Environment **24**:113–37.

Benson, S.M. 2005. Overview of Geologic Storage of CO_2. Pages 665–670 *in* S.M. Benson, editor. Carbon Dioxide Capture for Storage in Deep Geologic Formations – Results from the CO_2 Capture Project. Volume Two: Geologic Storage of Carbon Dioxide with Monitoring and Verification. Elsevier, Oxford, UK.

Doughty, C., Pruess, K. 2004. Modeling Supercritical Carbon Dioxide Injection in Heterogeneous Porous Media. Vadose Zone Journal 3:837–847.

Hayhoe, K., Cayan, D., Field, C., Frumhoff, P., Maurer, E., Miller, N., Moserh, S., Schneideri, S., Cahilld, K., Clelandd, E., Daleg, L., Drapekj, R., Hanemannk, R., Kalksteinl, L., Lenihanj, J., Lunchd, C., Neilsonj, R., Sheridanm, S., Vervillee, J. 2004. Emission Pathways, Climate Change, and Impacts on California. Proceedings of the National Academy of Sciences **101**:12422-12427.

Hillel, D., 1980. Fundamentals of Soil Physics. Academic Press, Inc. San Diego, CA.

Hove, A., Ringen, J., Read, P. 1985. Visualization of Laboratory Corefloods with the Aid of Computerized Tomography X-Rays. Paper 13654 presented to SPE California Regional Meeting, Bakersfield, March 1985. Society of Petroleum Engineers, Richardson, TX.

IPCC. 2001. Climate Change 2001: Mitigation. Contribution of Working Group III to the Third Assessment Report of the Intergovernmental Panel on Climate Change. B. Metz, et al., editors. Cambridge University Press, Cambridge, UK.

Marchetti, C. 1977. Geoengineering and the CO2 Problem. Climate Change 1: 97-68.

Mualem, Y. 1976. New Model for Predicting Hydraulic Conductivity of Unsaturated Porous-Media. Water Resources Research **12**:513-522.

Scheidegger, A. 1974. The Physics of Flow Through Porous Media. University of Toronto Press. Toronto.

van der Zwaan, B., Rabl, A. 2003. Prospects for PV: A learning curve analysis. Solar Energy **74**:19-31.

van Genuchten, M. 1980. A Closed-Form Equation for Predicting the Hydraulic Conductivity of Unsaturated Soils. Soil Science Society Of America Journal **44**:892-298.

Wuebbles, D., Jain, A., Edmonds, J., Harvey, D., Hayhoe, K. 1999. Global Change: State of Science. Environmental Pollution **100**:57-86.

Appendix A. Technical Glossary

Combined Cycle: a method of electricity generation where both gas and steam turbine cycles produce electricity in a single power plant. When a gaseous fuel is combusted, its expansion can drive a second turbine cycle in addition to the primary steam turbine.

Effective Permeability: the permeability of a porous substance to a single fluid when two fluids are present. The sum of the effective permeabilities of two fluids in a sandstone core equal the intrinsic permeability.

Intrinsic Permeability: the permeability of a porous substance to a single fluid.

Porosity: the fraction of the total mineral volume occupied by pore-space.

Relative Permeability: the ratio of effective permeability of a particular fluid at a particular saturation to intrinsic permeability of that fluid when it is the only fluid present. If a single fluid is present in a rock, its relative permeability is 1.0. Calculation of relative permeability allows comparison of the different abilities of fluids to flow in the presence of each other, since the presence of more than one fluid generally inhibits flow.

Saturation: Unlike the saturation of a solute in a solvent, in this paper, saturation refers to percent of the pore-space occupied by either CO_2 or brine. A brine-saturated core, therefore, has all its pore-space filled with brine.

Wettability: the preference of a solid to contact one liquid or gas rather than another, in what is known as the wetting phase.

Appendix B

CT scanning will be used to determine the distribution of CO_2 in the pore-spaces and the movement of CO_2 as it passes through the core during injection.

The following four steps describe the procedure for the relative permeability measurements. Parts B through D must be performed for each trial:

A. Construct multiple media core-flood apparatus.

B. Prepare and saturate core with CO_2-saturated brine at 7 MPa.

C. Inject liquid CO_2 into inlet of core.

D. Perform CT scans of core once equilibrium is reached.

A. Construction of Multiple Media Core-flood Apparatus The experimental apparatus (Figure 6) is centered on a horizontally oriented Berea sandstone core contained within a Phoenix Precision aluminum core holder. The core is encased in an impermeable rubber confining sleeve. Six ISCO pumps mix the necessary media and deliver liquid CO_2, brine (0.5M KI), CO_2-saturated brine, and CO_2 gas to the inlet of the core as needed. All pumps have independent Swagelock valves that control the flow of material through 1/6 inch stainless steel lines.

At the output end of the core holder, an overburden pump collects material passed through the core and maintains an internal pressure of 6.89 MPa, a pressure gauge provides visual confirmation of core holder pressure, and a Rosemount pressure transducer records this pressure with respect to time on a computer.

The CT scanner is used to take cross-sectional images of the core to measure relative concentration of liquid CO_2 and brine.

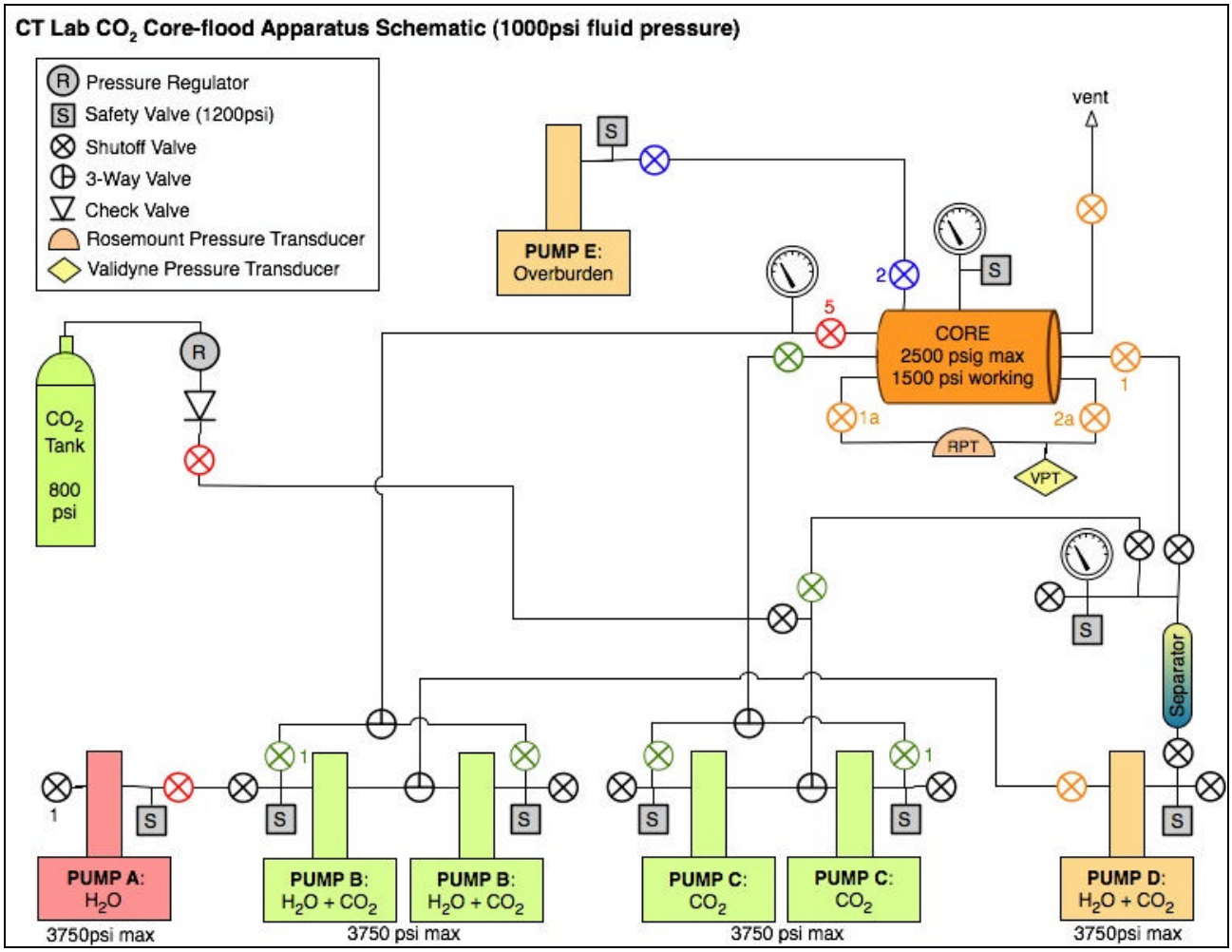

Figure 6. Detailed schematic of CO_2 core flooding apparatus.

B. Preparation and Saturation of Core with CO_2-saturated Brine The following steps were taken to prepare the core for liquid CO_2 and brine injection. The goal of this step was to achieve a core with its pore spaces completely filled with CO_2-saturated brine and no other gases.

i. Evacuate air from core.

ii. Flush core with $CO_{2(g)}$ to push out any residual air.

iii. Evacuate core again to remove $CO_{2(g)}$.

iv. Perform CT scan of "dry" core as baseline. (Method indicated in part D.)

v. Flush core with 20 pore volumes of non-CO_2-saturated brine: All pore space should be filled with brine and any remaining $CO_{2(g)}$ will be dissolved. Brine consists of 5% Potassium Iodide.

vi. Displace initial brine with 10 pore volumes of CO_2-saturated brine: CO_2 saturation prevents subsequently injected liquid CO_2 from dissolving into the brine and contaminating the results.

vii. Perform CT scan of fully brine-saturated core for second baseline by methods indicated in part D.

The core will then be completely filled with CO_2-saturated brine, confined at 9.65 MPa, and ready for liquid CO_2 and brine injection.

C. Injection of Liquid CO_2 and Brine into Inlet of Core Liquid CO_2 and brine will be injected into the core inlet in various proportions, as described in step one of the methods, and driven through the core at a constant flow rate of 3mL/minute by the pump. Internal pressure will be held constant by the overburden pump.

D. Perform CT Scans of Core Once Equilibrium is Reached Because brine and CO_2 attenuate x-rays differently, cross-sectional images of the two phases indicate the relative concentrations of brine and liquid CO_2 (Hove et al. 1985). Scan "slices" will be taken at 3mm intervals (the lateral resolution of the CT scanner) along the entire length of the core once the position of CO_2 and brine appear not to be changing.